

Computer simulation of trails on a square lattice. II. Finite temperatures and the collapse transition

H. Meirovitch and H. A. Lim

Supercomputer Computations Research Institute, Florida State University, Tallahassee, Florida 32306-4052

(Received 25 July 1988)

We study by the scanning simulation method trails on a square lattice at finite temperatures. This method constitutes a very efficient tool since it enables one to obtain results at *many* temperatures from a *single* sample generated at any given temperature. The tricritical temperature at which the collapse transition occurs is $-\varepsilon/k_B T_c = 1.086 \pm 0.002$. The tricritical exponents of the trail shape and its free energy are, respectively, $\nu_c = 0.569 \pm 0.008$ and $\gamma_c = 1.133 \pm 0.024$ (95% confidence limits). They are equal within the error bars to the exact values of self-attracting self-avoiding walks (SAW's). However, the crossover exponent $\phi_c = 0.807 \pm 0.005$ is significantly larger than the exact value 0.423 of SAW's. We also carry out a detailed scaling analysis near T_c and demonstrate that the various properties scale as predicted by theory. At sufficiently low temperatures ($T \leq T_c$) the persistence length appears to be ~ 1 .

I. INTRODUCTION

In the preceding paper¹ (hereafter referred to as paper I), we have described the scanning simulation method²⁻⁴ as applied to trails and have studied trails on a square lattice at temperature $T = \infty$ (i.e., trails without self-interactions). We have found that the shape exponent ν and the free energy exponent γ are equal, within relatively small statistical errors, to the corresponding exact values of self-avoiding walks (SAW's), which suggests that the two models belong to the same universality class. In the present paper (paper II), we apply the same method to trails on a square lattice at finite temperatures, where the attraction ε ($\varepsilon = -|\varepsilon|$) associated with each chain self-intersection, becomes effective. At high temperatures, one would expect the trail shape to be swollen, i.e., $\nu = 0.75$ like at $T = \infty$. However, below a certain temperature $T = T_c$, the chain is expected to collapse, which means that ν decreases sharply to $\nu = 1/D$ where $D = 2$ is the dimensionality. A similar picture is also expected in 3D and thus self-attracting trails, like self-attracting SAW's, may serve as a model for a dilute polymer system under various solvent conditions. The high-temperature regime mimics a polymer in a good solvent, whereas the transition region corresponds to the Flory Θ region^{5,6} at which a polymer in a poor solvent exhibits a Gaussian behavior. For self-attracting SAW's T_c has been identified by de Gennes⁷⁻⁹ as a tricritical point¹⁰⁻¹² for which the upper critical dimension is 3 and therefore in 2D, a non-Gaussian behavior is expected with nonclassical values of the various exponents. The collapsed transition has been studied extensively in 2D and 3D by various techniques;¹³⁻²⁴ recently, Duplantier and Saleur²⁵ have obtained the tricritical exponents analytically for the hexagonal lattice by a derivation which is conjectured to be exact (however, see also Refs. 26-30). The model of self-attracting trails was first introduced by Massih and Moore³¹ who solved it analytically on a special Bethe lat-

tice and studied the properties of the collapse transition. Shapir and Ono³² have later analyzed this transition by renormalization group techniques and have suggested to identify it as a tricritical point; however, they could not determine the universality class of trails at tricriticality. In order to elucidate this situation, Shapir and co-workers have recently carried out an extensive study of trails at tricriticality in 2D and 3D by exact enumeration; unfortunately, their chains of $N \leq 21$ steps appear to be too short to provide unequivocal conclusions.³³⁻³⁷ Hence we have decided to investigate much longer trails ($N = 300$) on a square lattice using the scanning method. We demonstrate that the method enables one to search very efficiently a large range of temperatures and, in particular, to locate T_c and to estimate the various exponents with high accuracy. We carry out a detailed scaling analysis of various properties close to T_c and, as in paper I, also study the persistence length. We rely heavily on the theory of the scanning method developed in paper I.

II. RESULTS AND DISCUSSION

A. Efficiency of the scanning method

We generate on the square lattice trails of $N = 300$ steps employing a scanning parameter $b = 4$; as in paper I, results are also calculated for the 30 partial chains of lengths $N = 10, 20, \dots$, and 300. At finite temperatures, we use the general scanning procedure which takes into account the interaction energy ε associated with each chain intersection (see Secs. II-V of paper I). In order to investigate the behavior of trails over a large range of temperatures and, in particular, to locate the tricritical temperature T_c , many simulations are required, which would make the study very time consuming. Fortunately, with the scanning method, such a search becomes a relatively simple task since one can obtain results at

many different temperatures from a *single* sample simulated at *any* given temperature. This can be seen, for example, from the importance sampling equation of the free energy \bar{F}_{IS} [Eq. (26) of paper I, abbreviated as (I.26), e.g.], which will be written again in a more general form,

$$\bar{F}_{\text{IS}}(T) = -k_B T \ln \left[W_0^{-1} \sum_{i=1}^n \exp \left(\frac{-E_{i(t)}}{k_B T} \right) / P_{i(t)} \right]. \quad (1)$$

The right-hand side of this equation leads to the correct free energy at temperature T from a sample generated with an *arbitrary* probability distribution P_i , which is not necessarily defined by the scanning method. Obviously, if $P_i = P_i(b, T_1)$, where $P_i(b, T_1)$ is obtained by a scanning construction at T_1 , which differs significantly from T , $P_i(b, T_1)$ might be strongly biased (with respect to the exact Boltzmann probability at T , P_i^B [Eq. (I.3)]) and the efficiency of the importance sampling procedure will become low or, equivalently, the acceptance rate [see Eq. (I.30)] will be small. Therefore one should study temperatures T , which are close enough to T_1 , the temperature at which the sample is produced. In this work, we have generated several samples at different temperatures T_1 and have studied in most cases from each such sample $n_T = 10$ different temperatures in the vicinity of T_1 . For example, in the hot region, for $K_1 = -\varepsilon/k_B T_1 = 0.25$, the temperatures studied are $K = K_{\min} = 0, 0.05, 0.1, \dots$, and $K_{\max} = 0.5$. For $K_1 = 1.080$ (close to the reciprocal

tricritical temperature), we have studied the temperatures $K = K_{\min} = 1.070, 1.072, \dots$, and $K_{\max} = 1.088$ and, in the cold region, for $K_1 = 1.3$, $K_{\min} = 1.175$, and $K_{\max} = 1.4$. However, the results for the acceptance rate R_I [Eq. (I.30)] for K_{\min} and K_{\max} (see Table I) are very close to those obtained for K_1 which means that a much larger range of temperatures can be studied from each single sample. In fact, only three samples are required to cover the range of temperatures of interest. Since most of the computer time is spent on calculating the transition probabilities at each step of the scanning construction, we do not see any limitation in increasing n_T to 50 or even more. The only problem which might arise in some cases is the large disk space required for the $30 \times n_T$ different sets of results for the n_T temperatures and the 30 partial trails. Therefore, as far as the search over the temperatures is concerned, the scanning procedure might be ~ 50 times more efficient than any simulation technique which does not provide the probability of construction (such as the Metropolis Monte Carlo method^{16,38,39}) and for which therefore a different simulation has to be carried out at each temperature of interest. [It should be pointed out that Eisenrigler, Kremer, and Binder⁴⁰ were the first to study many temperatures from a *single* sample by employing a biased technique which is different from the scanning method (see also Ref. 4)]. Table I reveals that, as expected, for each temperature K_1 the acceptance rate R_I [(Eq. (I.30)], decreases with increasing N ; also, for $N = 180$, R_I increases (even though only slightly)

TABLE I. Results at various reciprocal temperatures $K = -\varepsilon/k_B T$ and chain length N for the acceptance rate R_I [Eq. (I.30)], the approximate free energy $\bar{F}(b)$ [Eq. (I.22)], the free energy estimated by importance sampling \bar{F}_{IS} [Eq. (I.26)], the approximate radius of gyration $\bar{G}^2(b)$ [Eqs. (I.9), (I.10), and (I.21)], and that estimated by importance sampling \bar{G}_{IS}^2 [Eq. (I.25)]. K_1 is the temperature at which the simulation has been carried out; from this sample, results have been obtained for ten different temperatures in the range $[K_{\min}, K_{\max}]$. The statistical error of R_I is not larger than ± 0.01 , that of $\bar{F}(b)$ and \bar{F}_{IS} is smaller than ± 0.00008 and for $\bar{G}^2(b)$ and \bar{G}_{IS}^2 , the error is not larger than ± 0.005 (all errors one standard deviation).

| N | $R_I(K_1)$ | $R_I(K_{\min})$ | $R_I(K_{\max})$ | $-\bar{F}(b)/Nk_B T$ | $-\bar{F}_{\text{IS}}/Nk_B T$ | $\bar{G}^2(b)/N$ | \bar{G}_{IS}^2/N |
|---|------------|-----------------|-----------------|----------------------|-------------------------------|------------------|---------------------------|
| $K_1 = 0.03, K_{\min} = 0, K_{\max} = 0.05$ | | | | | | | |
| 90 | 0.35 | 0.35 | 0.36 | 1.008 18 | 1.021 69 | 0.566 | 0.825 |
| 180 | 0.12 | 0.11 | 0.12 | 0.989 99 | 1.013 13 | 0.627 | 1.14 |
| $K_1 = 0.25, K_{\min} = 0.05, K_{\max} = 0.50$ | | | | | | | |
| 90 | 0.35 | 0.27 | 0.40 | 1.017 55 | 1.030 79 | 0.525 | 0.769 |
| 180 | 0.11 | 0.07 | 0.17 | 0.999 92 | 1.022 23 | 0.577 | 1.05 |
| $K_1 = 1.00, K_{\min} = 0.95, K_{\max} = 1.04$ | | | | | | | |
| 90 | 0.35 | 0.30 | 0.38 | 1.082 52 | 1.092 77 | 0.327 | 0.432 |
| 180 | 0.15 | 0.11 | 0.19 | 1.074 59 | 1.086 55 | 0.334 | 0.518 |
| $K_1 = 1.080, K_{\min} = 1.070, K_{\max} = 1.088$ | | | | | | | |
| 90 | 0.34 | 0.33 | 0.35 | 1.094 70 | 1.104 78 | 0.303 | 0.379 |
| 180 | 0.17 | 0.16 | 0.17 | 1.089 23 | 1.100 00 | 0.308 | 0.421 |
| $K_1 = 1.3, K_{\min} = 1.175, K_{\max} = 1.4$ | | | | | | | |
| 90 | 0.27 | 0.21 | 0.21 | 1.134 25 | 1.147 24 | 0.248 | 0.243 |
| 180 | 0.09 | 0.07 | 0.05 | 1.136 43 | 1.151 71 | 0.248 | 0.189 |

TABLE II. Results for the acceptance rate R_I and the effective sample size n_{accept} , for various chain lengths N , at the tricritical temperature ($K_I = 1.086$).

| N | R_I | $n_{\text{accept}}/1000$ |
|-----|-------|--------------------------|
| 60 | 0.45 | 1924 |
| 120 | 0.27 | 743 |
| 180 | 0.17 | 468 |
| 240 | 0.11 | 303 |
| 300 | 0.07 | 193 |

from 0.11 to 0.17 in going from $K_1 = 0.03$ to 1.080. This is probably because close to K_I , the attractive and the repulsive interactions cancel each other to a large extent and the model can be handled more efficiently by the scanning method. It is also worth pointing out that in the hot region (i.e., at $K \leq 1.080$), $R_I(K_{\text{max}}) > R_I(K_1) > R_I(K_{\text{min}})$. This stems from the fact that the scanning construction at K_1 gives too high probability to the compact configurations, which, however, constitute the typical equilibrium ones at lower temperatures ($K > K_1$); therefore $P_i(K_1, b)$ is a better approximation for the Boltzmann probability $P_i^B(K_{\text{max}})$ than for $P_i^B(K_1)$ [see Eq. (I.3)]. Indeed, the approximate results of the radius of gyration $\bar{G}^2(b)$ [Eq. (I.24)] in the hot region ($K < K_I$) in Table I are always smaller than the importance sampling values \bar{G}_{IS}^2 [Eq. (I.25)], which are considered to be exact. Also, the ratio $\bar{G}_{\text{IS}}^2/\bar{G}^2(b)$ decreases in going from $K = 0.03$ to 1.080 from 1.45 to 1.25 and from 1.82 to 1.37 for $N = 90$ and 180, respectively. A similar be-

havior is found for the ratio of the free energies $\bar{F}_{\text{IS}}/\bar{F}(b)$. These last results demonstrate again that close to T_I , the scanning method leads to less biased probabilities than at high temperatures. At low temperatures ($K > K_I$), the scanning procedure gives too large (small) preference to the open (compact) configurations, which again is demonstrated in Table I by the inequality $\bar{G}^2(b) > \bar{G}_{\text{IS}}^2$.

In this work, we are especially interested in locating the tricritical temperature and in calculating the tricritical exponents; therefore a relatively large sample has been generated at $K = 1.080$ and results have been obtained for the 13 values of K (1.070, 1.072, . . . , and 1.094). We have generated a sample of $W_0 = 4\,275\,000$ attempted trails [see Eq. (I.16)], which required altogether 66 h of the CYBER205 and ETA¹⁰ supercomputers. For this problem, the ETA¹⁰ has been found to be more efficient than the CYBER205 by $\sim 18\%$ (we used the scalar optimizers in both machines). This code runs 2.5 times slower on the VAX 8700 computer. At low temperatures, where the compact configurations become the typical equilibrium ones, the probability that a trail will come to a dead end during construction (i.e., it will visit the origin three times) increases and therefore the attrition factor A (i.e., the fraction of trails succeeded [Eq. (I.16)]) decreases as compared to $T = \infty$. However, even for $N = 300$ at $K = 1.086$, A is relatively large, $A > 0.96$. In Table II we provide the acceptance rates and the sample sizes for several chain lengths N at $K_I = 1.086$ (which is found to be the reciprocal tricritical temperature, see

TABLE III. Results for the autocorrelation functions ρ [Eq. (I.33)] of the approximate probability $\ln P_i(b=4)$ [Eq. (I.15)], the energy E_i [Eq. (I.1)], the square end-to-end distance R_i^2 , and the square radius of gyration G_i^2 at different temperatures. K and R_I are defined in the captions of Tables I and II. The statistical error is smaller than ± 0.01 (one standard deviation).

| t | $\rho_{\ln P(b)}(t)$ | $\rho_E(t)$ | $\rho_{R^2}(t)$ | $\rho_{G^2}(t)$ |
|----------------------------------|----------------------|-------------|-----------------|-----------------|
| $K = 0.05, N = 120, R_I = 0.17$ | | | | |
| 1 | 0.42 | 0.19 | 0.05 | 0.11 |
| 2 | 0.17 | 0.09 | 0.01 | 0.05 |
| 3 | 0.07 | 0.04 | | 0.02 |
| 4 | 0.03 | 0.02 | | |
| $K = 0.95, N = 120, R_I = 0.21$ | | | | |
| 1 | 0.25 | 0.17 | 0.04 | 0.07 |
| 2 | 0.11 | 0.08 | 0.01 | 0.03 |
| 3 | 0.05 | 0.04 | | 0.02 |
| 4 | 0.01 | 0.01 | | |
| $K = 1.086, N = 120, R_I = 0.25$ | | | | |
| 1 | 0.11 | 0.06 | 0.01 | 0.01 |
| 2 | 0.05 | 0.03 | | |
| 3 | 0.02 | 0.01 | | |
| $K = 1.3, N = 120, R_I = 0.19$ | | | | |
| 1 | 0.02 | 0.01 | 0.0 | 0.0 |
| $K = 1.55, N = 100, R_I = 0.14$ | | | | |
| 1 | 0.08 | 0.17 | 0.07 | 0.12 |
| 2 | 0.04 | 0.08 | 0.03 | 0.06 |
| 3 | 0.02 | 0.04 | 0.02 | 0.03 |

Sec. II B). It should be noticed that because of the larger acceptance rate at this temperature than at $T = \infty$, the sizes of the accepted samples n_{accept} are significantly larger here than in Table II of paper I, even though the number of attempted trails W_0 is larger in paper I than here. Using the results for R_l in Table II we have obtained by a least-squares procedure the values of the acceptance constant λ and the prefactor D [see Eq. (I.30)] at $K_t = 1.086$,

$$\lambda \sim 0.0077, \quad D \sim 0.696.$$

Since $A > 0.96$, the amount of computation required for generating an N -step trail grows approximately linearly with N (see also discussion in Sec. VI A of paper I). However, the number of accepted trails decreases exponentially with increasing N with the above acceptance constant. It should be noticed that $\lambda(K_t) < \lambda(K=0) \sim 0.013$ and $D(K_t) < D(K=0) \sim 1.08$. This means that the simulation is more efficient at the tricritical point than at $T = \infty$ ($K=0$). Similar calculations based on the values of R_l for different temperatures K_1 in Table I show that λ decreases gradually as K_1 increases from $K_1=0$ to K_t . However, as K_1 is further increased to $K_1=1.3$ (cold region), λ increases again to 0.012, which means that the simulation becomes less efficient.

The autocorrelation functions ρ [Eq. (I.33)] of $\ln P_i(b)$, the energy E_i , the square end-to-end distance R_i^2 , and the square radius of gyration G_i^2 for several temperatures are shown in Table III. The table reveals that R_i^2 is always uncorrelated, G_i^2 is slightly correlated at high and low temperatures [$\rho_{G^2}(t=1) \sim 0.1$] and becomes uncorrelated in the tricritical region. One would expect the function $F_i/k_B T = E_i/k_B T + \ln P_i(b)$, and each of its ingredients, E_i and $\ln P_i(b)$, to be correlated, since they define the transition probabilities A_{ij} of the Schmidt procedure [Eq. (I.29)]. Indeed, the table shows that at high temperature, they all are correlated where for $t=1$ $\rho_{\ln P(b)}$ is significantly larger than ρ_E due to the fact that $\ln P_i(b)$ is much larger than $E_i/k_B T$. In the tricritical region $F_i/k_B T$ is still correlated (i.e., F_j is close to or smaller than F_i for a trail j which is accepted after trail i); how-

ever, $E_i/k_B T$ and $\ln P_i$ become comparable and therefore the values of E_i and E_j might differ significantly from each other due to a compensation of the corresponding values of $\ln P_i(b)$ and $\ln P_j(b)$; hence the autocorrelations of both E_i and $\ln P_i(b)$ vanish. At very low temperatures, E_i dominates $\ln P_i(b)$ and its autocorrelations become significant and larger than those of $\ln P_i$ (in contrast to the picture found at high temperatures). This means that for a wide range of temperatures around T_t , n_{accept} can be considered as the effective sample size for all the quantities of interest (see discussion in Sec. VI A of paper I).

B. Tricritical temperature

The tricritical temperature T_t can conveniently be located from the results of the radius of gyration G or the end-to-end distance R close to T_t . One may adopt for trails the generalized scaling behavior assumed for SAW's at tricriticality^{8-12, 15, 16}

$$G_N \equiv \langle G^2 \rangle^{1/2} = N^{\nu_t} f_{\pm}(N^{\phi_t} \tau), \quad (2)$$

where ϕ_t is a crossover exponent and $\tau = |T - T_t|/T_t$. For small τ and large x (i.e., large N), f_{\pm} must have the form

$$f_{\pm}(x) \sim x^{\mu} \begin{cases} \mu = \mu^+ = (\nu - \nu_t)/\phi_t, & T > T_t \\ \mu = 0, & T = T_t \\ \mu = \mu^- = (\frac{1}{2} - \nu_t)/\phi_t, & T < T_t \end{cases} \quad (3)$$

which means that long enough trails at $T > T_t$ will always be swollen, i.e., the shape will be characterized by $\nu = 0.75$ while at $T < T_t$ they will collapse, i.e., $\nu = \frac{1}{2}$. However, short trails at $T > T_t$ will expand with $\nu < 0.75$ which is expected to increase monotonically and approach 0.75 for very large N . An opposite trend is expected at $T < T_t$, where the shape of the shorter chains grows with $\nu > \frac{1}{2}$, which decreases asymptotically to $\frac{1}{2}$. Thus at $T = T_t$, $\nu_t(N)$ is expected to become flat, i.e., independent of N . It should be noted that Eqs. (2) and (3) also hold for the end-to-end distance R_N where R and R_N replace G and G_N , respectively; we will denote (as in pa-

TABLE IV. Results for the exponents ν_G (radius of gyration), ν_R (end-to-end distance), and y (specific heat) obtained by a least-squares procedure based on the importance sampling results of \bar{G}_{IS}^2 , \bar{R}_{IS}^2 , and \bar{C}_{IS} [Eq. (I.25)], respectively, and on Eqs. (2) and (3) for several subchains at various temperatures K around the tricritical point. Δ_G^2 is the sum of the deviations (squared) per step of the "experimental" results for $\ln G_N$ [Eq. (2)] from those defined by the best-fitted straight line for $\ln G_N$ vs $\ln N$; Δ_R^2 is calculated for the end-to-end distance. The smallest values of Δ are indicated with an asterisk.

| $-\epsilon/k_B T$ | Subchain (N) | ν_G | | $10^3 \Delta_G$ | ν_R | | $10^3 \Delta_R$ | y |
|-------------------|------------------|---------|---------|-----------------|---------|---------|-----------------|--------|
| | | 30-110 | 110-220 | 30-220 | 30-110 | 110-220 | 30-220 | 50-260 |
| 1.078 | | 0.566 | 0.570 | 0.649 | 0.576 | 0.583 | 6.31 | 0.600 |
| 1.080 | | 0.565 | 0.568 | 0.559 | 0.575 | 0.581 | 5.73 | 0.604 |
| 1.082 | | 0.564 | 0.566 | 0.479 | 0.574 | 0.578 | 5.20 | 0.608 |
| 1.084 | | 0.563 | 0.564 | 0.418 | 0.573 | 0.576 | 4.75 | 0.610 |
| 1.086 | | 0.562 | 0.562 | 0.386* | 0.572 | 0.574 | 4.41 | 0.614 |
| 1.088 | | 0.560 | 0.560 | 0.390 | 0.570 | 0.571 | 4.21* | 0.618 |
| 1.090 | | 0.559 | 0.556 | 0.598 | 0.569 | 0.568 | 5.38 | 0.624 |
| 1.092 | | 0.558 | 0.554 | 0.679 | 0.568 | 0.565 | 5.53 | 0.626 |

per I) the results for ν obtained from the radius of gyration and the end-to-end distance by ν_G and ν_R , respectively. Thus calculating the ν values of several subchains at different temperatures (assuming $G_N \sim N^\nu$) enables one to locate T_t on the basis of the above flatness criterion. Such results are presented in Table IV. They have been obtained from a large single sample generated at $K = -\varepsilon/k_B T = 1.080$ as has been discussed in Sec. II A. The table reveals that for each $K < 1.084$, the value of ν of the second subchain [$\nu(2)$] is larger than that obtained for the first time [$\nu(1)$] and that $\nu(1) \rightarrow \nu(2)$ as K approaches 1.084; these temperatures, therefore, belong to the hot region. An opposite trend [i.e., $\nu(1) > \nu(2)$] is observed for $K > 1.088$ and hence these temperatures pertain to the cold region. For $1.084 \leq K \leq 1.088$, $\nu(1)$ and $\nu(2)$ become equal which suggests that $K_t = 1.086 \pm 0.002$. This value of K_t is also obtained by another criterion: it corresponds to the minimal value of Δ^2 , where Δ^2 is the sum of the deviations (squared) per step of the "experimental" values of $\ln G_N$ ($30 \leq N \leq 220$) from those defined by the best-fitted straight line for $\ln G_N$ vs $\ln N$. A similar analysis of the results for the end-to-end distance R_N leads to $K_t \approx 1.088$. At this point, the following remarks should be made. (1) In the above analysis, only results for $N \leq 220$ are taken into account since those for the longer trails appear to be less accurate due to insufficient statistics (see Figs. 1 and 2). (2) The shortest trails considered are of $N = 30$ since for $N < 30$, the shape of the trails is found to be affected by the chain stiffness (see discussion in Ref. 16). (3) The results in Table IV for the different values of K change within their statistical error ranges in a correlated way due to the fact that they are obtained from the same *single* sample. (4) In order to determine K_t , we rely on the results for G , which are more accurate than those of R . Our analysis is based on calculation of many tables similar to Table IV for different subchains and also for partial samples, even smaller than those defined in Sec. VI B in paper I. In all of these calculations, K_t has always been found to fall in the range $1.084 \leq K_t \leq 1.088$, which suggests that the following error bars are of 95% confidence

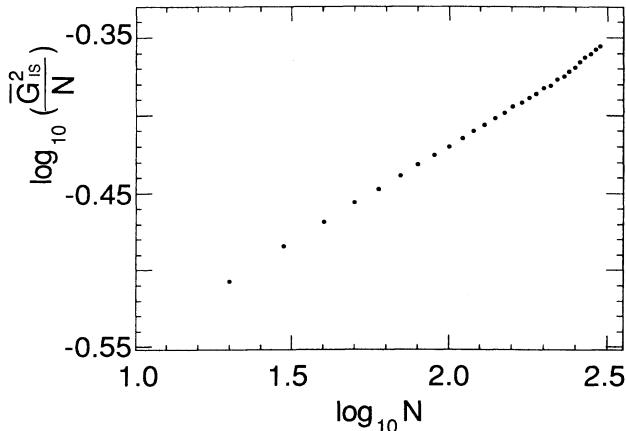


FIG. 1. Log-log plot of the importance sampling results (at the tricritical temperature $-\varepsilon/k_B T_t = 1.086$) of the square radius of gyration \bar{G}_{is}^2 vs chain length N .

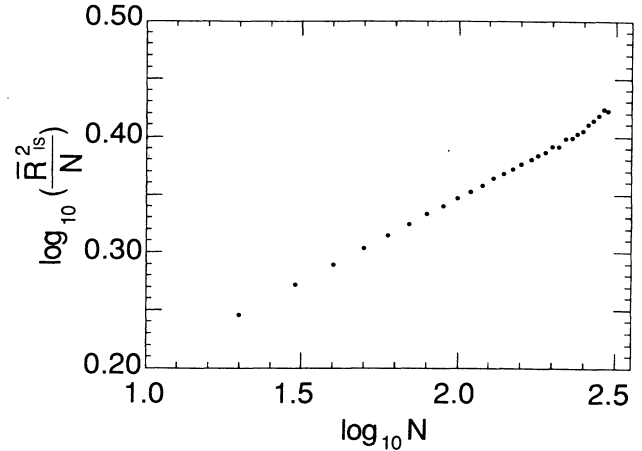


FIG. 2. Log-log plot similar to that of Fig. 1, but for \bar{R}_{is}^2 , the square end-to-end distance.

limits,

$$K_t = -\varepsilon/k_B T = 1.086 \pm 0.002 ,$$

$$\nu_t(G) = 0.563 \pm 0.003, \quad \nu_t(R) = 0.574 \pm 0.005 .$$

The error bars for ν_t (95% confidence limits) take into account the uncertainty in the value of K_t . This estimate of K_t differs significantly from the value $K_t = 1.55$ obtained by exact enumeration³⁵ of relatively short trails, $N \leq 21$. Again, like for trails at $T = \infty$ (see paper I) $\nu_t(R) > \nu_t(G)$. Obviously, one would expect that asymptotically $\nu_t(G) = \nu_t(R)$. However, the average of these values of ν_t , 0.569, is equal (within the statistical errors) to the analytical value $\nu_t = \frac{4}{7} = 0.571 \dots$ obtained by Duplantier and Saleur²⁵ for self-attracting SAW's and which is conjectured to be exact.

In order to calculate the crossover exponent ϕ_t , we analyze the results of the specific heat per step $C(T, N)$ which are calculated from the fluctuation of the energy

$$C(T, N)/k_B = \frac{\varepsilon^2}{k_B^2 T^2 N} (\langle m^2 \rangle - \langle m \rangle^2) , \quad (4)$$

where the energy $E_i = \varepsilon m_i$ [see Eq. (I.1)]. Close to T_t , $C(T, N)$ is expected to scale like

$$C(T, N) = N^{-y_t} g(N^{\phi_t} \tau) , \quad (5)$$

where $y_t = \alpha_t \phi_t$ and α_t is the tricritical exponent of the specific heat. For large x (small τ),

$$g(x) \sim \begin{cases} A^+ x^{-\alpha_t}, & T > T_t \\ \text{const}, & T = T_t \\ A^- x^{-\alpha_t}, & T < T_t \end{cases} \quad (6)$$

where A^+ and A^- are prefactors. Thus one can calculate the exponent y_t from the results of C at T_t by a least-squares procedure. In Table IV, the results for y are shown for different values of K . They are based on the range $50 \leq N \leq 260$ in which the results for C appear to be statistically most reliable (see Fig. 3). We obtain

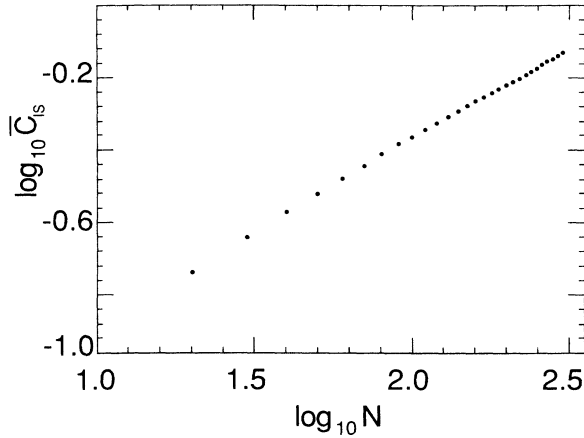


FIG. 3. Log-log plot similar to that of Fig. 1, but for \bar{C}_{1s} , the specific heat per step.

$$y_t = 0.614 \pm 0.008 .$$

One can use the relation⁴¹

$$\alpha_t = 2 - 1/\phi_t , \quad (7)$$

which leads to

$$\phi_t = (1 + y_t) / 2 . \quad (8)$$

Thus we find (95% confidence limits),

$$\phi_t = 0.807 \pm 0.005, \quad \alpha_t = 0.761 \pm 0.007 .$$

Our value for ϕ_t differs considerably from the theoretical value for self-attracting SAW's (Ref. 25) ($\phi_t = \frac{3}{7} = 0.423 \dots$) and it is slightly larger than a recent exact enumeration estimate³⁶ $\phi_t = 0.68 \pm 0.08$, obtained for trails on a triangular lattice. It should be pointed out that the theoretical value of α_t for SAW's is negative ($\alpha_t = -\frac{1}{3}$) which indicates the possibility of the existence of a cusp in the graph of $C(T, N \rightarrow \infty)$ versus T . However, such a cusp has not been observed in Baumgärtner's Monte-Carlo results of self-attracting SAW's of $N \leq 160$ on a square lattice¹⁵ and obviously it does not appear in the present simulation of trails of $N \leq 300$.

The tricritical temperature and ϕ_t can also be obtained from the behavior of $T_t(N)$, where $T_t(N)$ is the temperature at which the specific heat $C(T, N)$ of an N -step trail becomes maximal [obviously $T_t = T_t(N = \infty)$]. Thus one can assume the following behavior:^{15,16}

$$\frac{k_B}{\varepsilon} [T_t(\infty) - T_t(N)] \simeq N^{-\phi_t} , \quad (9)$$

from which both ϕ_t and T_t can be estimated by a least-squares best fit. Results for $C_{\max}(N)$, the maximal values of $C_N(T, N)$, appear in Table V. They are located in the cold region and approach K_t as N increases. In Table V, we also present the reciprocal temperatures $K_t(N) = -\varepsilon/k_B T_t(N)$ at which these maxima occur. Best fitting these results to Eq. (9) leads to

$$K_t = -\varepsilon/k_B T_t = 1.07 \pm 0.04, \quad \phi_t = 0.75 \pm 0.14 .$$

TABLE V. Importance sampling results for $C_{\max}(N)$, the maximal value of the specific heat of an N -step trail and for $K_t(N) = -\varepsilon/k_B T_t(N)$, the temperature at which the maximum occurs. The statistical error (one standard deviation) is not larger than ± 0.02 for $K_t(N)$ and ± 0.006 for $C_{\max}(N)$.

| N | $C_{\max}(N)$ | $K_t(N)$ |
|-----|---------------|----------|
| 60 | 0.489 | 1.550 |
| 70 | 0.520 | 1.460 |
| 80 | 0.536 | 1.450 |
| 90 | 0.558 | 1.375 |
| 100 | 0.580 | 1.350 |
| 110 | 0.604 | 1.318 |
| 120 | 0.622 | 1.312 |
| 130 | 0.640 | 1.310 |
| 140 | 0.664 | 1.275 |
| 150 | 0.685 | 1.270 |
| 160 | 0.710 | 1.259 |
| 170 | 0.724 | 1.250 |
| 180 | 0.750 | 1.230 |

These estimates agree with those calculated previously. However, the statistical errors here are larger because of the difficulty in locating the maxima of $C(T, N)$ and therefore the values of $K_t(N)$. These errors define the ranges in which the parameters K_t and ϕ_t change for partial sets of results of sizes 9 to 13 (see Table V).

C. Partition function

The partition function $Z(T)$ can be obtained by importance sampling as has been discussed in paper I [Eq. (I.36)]. For $T > T_t$, one expects $Z(T)$ to behave as $N^{\gamma-1} \mu^N(T)$ [see Eq. (I.36)] where the growth parameter $\mu(T)$ is a function of the temperature while γ is equal to $\gamma(T = \infty)$. However, at $T = T_t$, $\mu(T)$ as well as γ , are expected to attain their tricritical values γ_t ($\neq \gamma$) and μ_t , respectively. In order to estimate γ_t and μ_t , we take into account analytical correction to scaling, i.e.,

$$Z(T_t) = BN^{\gamma_t-1} \mu_t^N (1 + c/N) . \quad (10)$$

As in paper I (see Sec. VI C), we best fit our results for the free energy $\bar{F}_{1s}(N)$ [Eq. (I.26)] at $K_t = 1.086$ to Eq. (10) and employ the flatness criterion of Berretti and Sokal⁴² to obtain the optimized values of γ_t and μ_t . Results for $\gamma(N_{\min})$ and $\mu(N_{\min})$ are presented in Table VI for $20 \leq N_{\min} \leq 60$ and $N_{\max} = 240$, where the flattest graph is obtained for $c^* = -0.6$. Thus $\gamma(1.086) = 1.125 \pm 0.011 \pm 0.001$ (95% confidence limits) where the first and the second errors are the statistical and the systematic errors, respectively (see discussion in Secs. VIB and VIC of paper I). We have also calculated such tables for $180 \leq N_{\max} \leq 300$ and have found that the values of c^* (and of the corresponding values of γ and μ —denoted by γ^* and μ^*) are stable for $180 \leq N_{\max} \leq 240$, i.e., they fluctuate without any trend around their average value. (This stability has been found to hold also for larger values N_{\min} , $20 \leq N_{\min} \leq 80$). In Table VII, the results for c^* , γ^* , and μ^* are presented for $180 \leq N_{\max} \leq 240$ ($20 \leq N_{\min} \leq 60$). Our best estimates of γ_t and μ_t are ob-

TABLE VI. Sets of results for γ and μ as functions of N_{\min} for different values of the parameter c [see Eq. (10)] calculated at $K_t = 1.086$ for $N_{\max} = 240$. These results have been obtained by a least-squares procedure based on the importance sampling results of the free energy \bar{F}_{IS} and Eq. (10); Δ is the standard deviation of the results of each line. The flattest graphs (indicated by asterisks) are obtained for $c^* = -0.6$. (For details, see Secs. VIB and VIC of paper I.)

| c | N_{\min} | 20 | 30 | 40 | 50 | 60 | Δ | Average |
|-------|------------|---------|---------|---------|---------|---------|----------|---------|
| -0.9 | | 1.1158 | 1.1178 | 1.1192 | 1.1192 | 1.1199 | 0.00145 | 1.1184 |
| -0.8 | | 1.1191 | 1.1203 | 1.1214 | 1.1211 | 1.1217 | 0.00094 | 1.1207 |
| -0.7 | | 1.1223 | 1.1229 | 1.1235 | 1.1231 | 1.1234 | 0.00041 | 1.1230 |
| -0.6* | | 1.1256* | 1.1254* | 1.1257* | 1.1250* | 1.1251* | 0.00026* | 1.1254* |
| -0.5 | | 1.1287 | 1.1280 | 1.1278 | 1.1269 | 1.1269 | 0.00068 | 1.1277 |
| -0.4 | | 1.1319 | 1.1305 | 1.1300 | 1.1287 | 1.1286 | 0.00124 | 1.1299 |
| -0.3 | | 1.1350 | 1.1330 | 1.1321 | 1.1306 | 1.1303 | 0.00171 | 1.1322 |
| -0.2 | | 1.1382 | 1.1355 | 1.1343 | 1.1326 | 1.1320 | 0.00224 | 1.1345 |

| c | N_{\min} | 20 | 30 | 40 | 50 | 60 | Δ | Average |
|-------|------------|----------|----------|----------|----------|----------|------------|----------|
| -0.9 | | 2.99044 | 2.99039 | 2.99036 | 2.99036 | 2.99035 | 0.000033 | 2.99038 |
| -0.8 | | 2.99039 | 2.99036 | 2.99033 | 2.99034 | 2.99033 | 0.000216 | 2.99035 |
| -0.7 | | 2.99033 | 2.99032 | 2.99030 | 2.99031 | 2.99031 | 0.000009 | 2.99031 |
| -0.6* | | 2.99028* | 2.99028* | 2.99027* | 2.99029* | 2.99029* | 0.0000056* | 2.99028* |
| -0.5 | | 2.99023 | 2.99024 | 2.99025 | 2.99027 | 2.99027 | 0.000015 | 2.99025 |
| -0.4 | | 2.99017 | 2.99021 | 2.99022 | 2.99024 | 2.99025 | 0.000028 | 2.99022 |
| -0.3 | | 2.99012 | 2.99017 | 2.99019 | 2.99022 | 2.99023 | 0.000038 | 2.99019 |
| -0.2 | | 2.99007 | 2.99013 | 2.99016 | 2.99020 | 2.99021 | 0.000050 | 2.99015 |

tained by averaging these values. The errors are determined as in paper I in two ways: (a) we calculate tables similar to Table VI for $K_t = 1.088$ and 1.084 and obtain as above the values of $\gamma(1.088)$ and $\gamma(1.084)$ with the corresponding errors; (b) we calculate at these two temperatures tables like Table VII for the entire sample and for partial samples and calculate the standard deviation for μ and γ from their average values in Table VII. This leads to (95% confidence limits)

$$\gamma_t = 1.133 \pm 0.024, \quad \mu_t = 2.9901 \pm 0.0020.$$

This result for γ_t is equal (within the error bars) to the theoretical value $\frac{8}{7} = 1.1428 \dots$ obtained by Duplantier and Saleur²⁵ for self-attracting SAW's. Our results differ considerably from estimates of γ and μ obtained by exact enumeration of short trails on a square lattice.³⁵

TABLE VII. Results for the optimal values c^* , γ^* , and μ^* at $K_t = 1.086$ obtained by the flatness criterion at various values of N_{\max} (see Secs. VIB and VIC of paper I). The average values of γ^* and μ^* are also presented.

| N_{\max} | c^* | γ^* | μ^* |
|------------|-------|------------|---------|
| 180 | -0.5 | 1.129 | 2.9902 |
| 190 | -0.3 | 1.137 | 2.9900 |
| 200 | -0.2 | 1.140 | 2.9900 |
| 210 | -0.5 | 1.130 | 2.9902 |
| 220 | -0.3 | 1.136 | 2.9901 |
| 230 | -0.4 | 1.133 | 2.9901 |
| 240 | -0.6 | 1.125 | 2.9903 |
| Average | | 1.133 | 2.9901 |

D. Scaling analysis

In Figs. 4, 5, and 6 we examine the validity of the scaling functions $G_N^2/N^{2\nu_t}$ of the radius of gyration, $R_N^2/N^{2\nu_t}$ of the end-to-end distance [Eqs. (2) and (3)] and C/N^{ν_t} of the specific heat [Eqs. (5) and (6)] by log-log plotting the importance sampling results of these functions versus the scaling variable $N^{\phi_t}\tau$. These plots are based on our best estimates, $K_t = 1.086$ and $\phi_t = 0.807$.

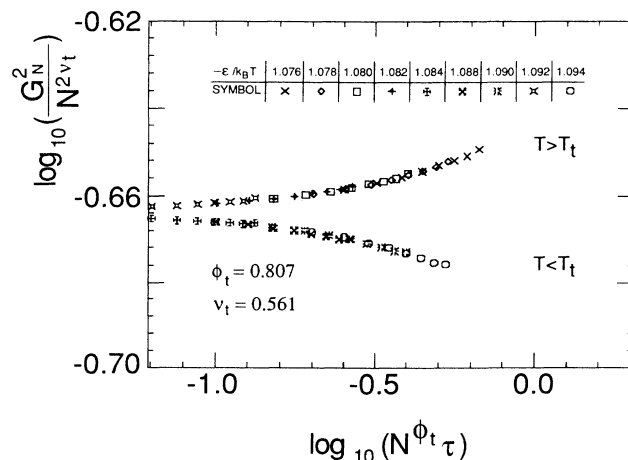


FIG. 4. Log-log plot of the importance sampling results of the scaling function of the square radius of gyration $G_N^2/N^{2\nu_t}$ vs the scaling variable $N^{\phi_t}\tau$ close to the tricritical temperature [see Eqs. (2) and (3)]. The chain length values are $N = 60, 80, \dots$, and 200.

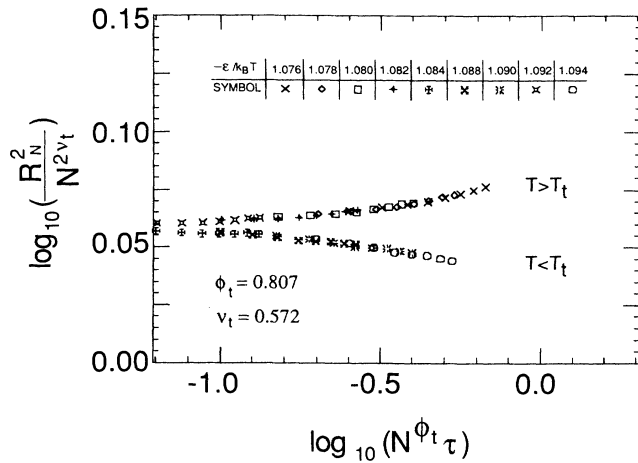


FIG. 5. Log-log plot similar to that of Fig. 4, but for the square end-to-end distance $R_N^2/N^{2\nu_t}$.

The range of K studied is $1.076 \leq K \leq 1.094$ for $N = 60, 80, \dots$, and 200. The figures show a very good scaling behavior. It should be pointed out, however, that this behavior depends strongly on the values of the exponents ν_t and ν_r , while it is less sensitive to the values of T_t and ϕ_t . In the figures, we have therefore employed the values $\nu_t(G) = 0.561$ and $\nu_t(R) = 0.572$ which have been found to lead to the best scaling behavior; they are located within the error bars of our best estimates obtained from Table IV. It should be noted that the asymptotic regime of the scaling functions has not yet been attained in these graphs since the values of N studied are too small.

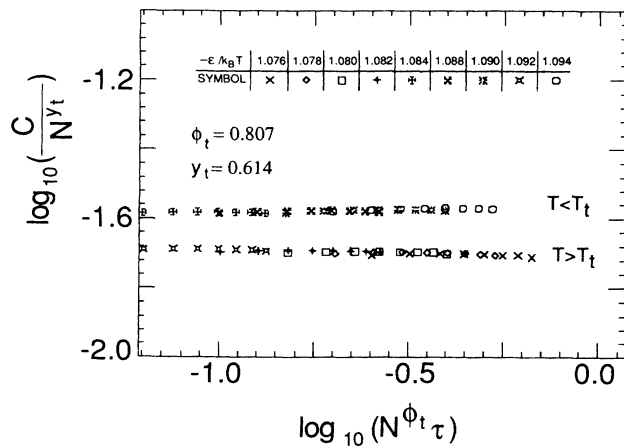


FIG. 6. Log-log plot similar to that of Fig. 4, but for the scaling function C/N^{ν_t} of the specific heat per step [see Eqs. (5) and (6)]. In order to demonstrate the scaling behavior at small τ the two branches have been separated.

TABLE VIII. Importance sampling results for the persistence length \bar{X}_{IS} as a function of the trail length N at various temperatures, $K = -\epsilon/k_B T$. The results denoted by an asterisk are the exact values obtained by exact enumeration (Ref. 43). For $N = 100$ at $K = 0.95$ and 1.40 and for $N = 160$ at $K = 1.086$ the statistical error is ± 0.08 (one standard deviation); this error decreases for the shorter trails due to larger samples of accepted trails.

| $N \backslash K$ | 0.950 | 1.086 | 1.40 |
|------------------|--------|--------|--------|
| 10 | 1.265 | 1.212 | 1.080 |
| | 1.263* | 1.206* | 1.070* |
| 20 | 1.224 | 1.162 | 1.030 |
| | 1.220* | 1.153* | 1.005* |
| 30 | 1.205 | 1.135 | 0.997 |
| 40 | 1.206 | 1.111 | 0.999 |
| 50 | 1.187 | 1.094 | 1.013 |
| 60 | 1.207 | 1.087 | 1.001 |
| 70 | 1.238 | 1.073 | 1.010 |
| 80 | 1.282 | 1.064 | 1.040 |
| 90 | 1.301 | 1.051 | 1.049 |
| 100 | 1.345 | 1.033 | 1.040 |
| 110 | | 1.037 | |
| 120 | | 1.029 | |
| 130 | | 1.033 | |
| 140 | | 1.038 | |
| 150 | | 1.055 | |
| 160 | | 1.061 | |

E. Persistence length

In Table VIII, the importance sampling results of the persistence length $\langle X \rangle$ [Eq. (I.11)] are presented for $K = 0.95$, $K_t = 1.086$, and $K = 1.4$. The statistical errors have been obtained from the values of $\langle Y \rangle$ (not shown in the table) and results for $\langle X \rangle$ which are based on partial samples (one standard deviation). It should be noticed that the exact enumeration results⁴³ for $N = 10$ and 20 are very close to the computer simulation estimates. The persistence length of an N -step trail is expected to decrease as the temperature is lowered since the typical equilibrium configurations become more compact; this indeed is demonstrated by the results in Table VIII. The table also reveals that at the coldest temperature ($K = 1.4$), \bar{X}_{IS} decreases from 1.080 to 0.997 as N goes from 10 to 30, and then it stabilizes around the value 1.0, which is the persistence length of a pure random walk.⁴⁴ This decrease of \bar{X}_{IS} is probably a result of the chain stiffness (caused by the restriction that an immediate chain reversal is forbidden) which has stronger effect on the shorter trails. At the tricritical temperature ($K_t = 1.086$), a similar behavior is observed, where \bar{X}_{IS} decreases monotonically from 1.212 to 1.033 in going from $N = 10$ to 100, and then increases up to 1.061 for $N = 160$. The results for $N > 160$ (not shown in the table) are unreliable since they are subject to a relatively large statistical error of up to ± 0.2 ; however, they strongly fluctuate (± 0.07) without any trend around their average value, 1.085. We therefore conclude that the persistence length of long trails is close to 1. Thus trails at K_t appear

to behave differently than at $T = \infty$ (see paper I), where $\langle X \rangle$ was found to increase with increasing N . At a hotter temperature ($K = 0.95$), a decrease of \bar{X}_{IS} for the shorter trails $10 < N \leq 50$ is again observed while for $60 \leq N \leq 100$, $\langle X \rangle$ increases. However, the data are not accurate enough to determine whether $\langle X \rangle$ converges to some value as N increases.

III. SUMMARY

We have studied by the scanning method trails on a square lattice at finite temperatures, in particular at the tricritical region. We have demonstrated that the method is very efficient for investigating a large range of temperatures. Our results for ν_i and γ_i are equal within

the statistical errors to the exact values derived by Duplantier and Saleur for self-attracting SAW's. However, our value of ϕ_i is significantly larger than that obtained for SAW's. This suggests that the two models do not belong to the same universality class. We also find that for $T \leq T_i$ the persistence length is close to 1.

ACKNOWLEDGMENTS

We thank Professor Y. Shapir for helpful discussions. We would also like to acknowledge support by the Florida State University Supercomputer Computations Research Institute which is partially funded by the U.S. Department of Energy under the Contract No. DE-FC05-85ER25000.

-
- ¹H. A. Lim and H. Meirovitch, preceding paper, *Phys. Rev. A* **39**, 4176 (1989).
²H. Meirovitch, *Phys. Rev. A* **32**, 3699 (1985).
³S. Livne and H. Meirovitch, *J. Chem. Phys.* **88**, 4498 (1988).
⁴H. Meirovitch and S. Livne, *J. Chem. Phys.* **88**, 4507 (1988).
⁵P. J. Flory, *Principles of Polymer Chemistry* (Cornell University Press, Ithaca, 1953).
⁶P. J. Flory, *J. Chem. Phys.* **17**, 303 (1949).
⁷P. G. de Gennes, *J. Phys. Lett. (Paris)* **36**, L55 (1975); **39**, L299 (1978).
⁸P. G. de Gennes, *Scaling Concepts in Polymer Physics* (Cornell University Press, Ithaca, 1985).
⁹M. Daoud and G. Jannink, *J. Phys. (Paris)* **37**, 973 (1976).
¹⁰R. B. Griffiths, *Phys. Rev. Lett.* **24**, 715 (1970); E. K. Riedel, *ibid.* **28**, 675 (1972).
¹¹I. D. Lewine and S. Sarbach, in *Phase Transition and Critical Phenomena*, edited by C. Domb and J. L. Lebowitz (Academic, London, 1985).
¹²M. J. Stephen and J. L. McCauley, Jr., *Phys. Lett.* **44A**, 89 (1973); M. J. Stephen, *ibid.* **53A**, 363 (1975).
¹³F. L. McCrackin, J. Mazur, and C. L. Guttman, *Macromolecules* **6**, 859 (1973).
¹⁴D. C. Rapaport, *J. Phys. A* **10**, 637 (1977).
¹⁵A. Baumgärtner, *J. Phys. (Paris)* **43**, 1407 (1982).
¹⁶K. Kremer, A. Baumgärtner, and K. Binder, *J. Phys. A* **15**, 2879 (1982).
¹⁷Vilanove and F. Rondelez, *Phys. Rev. Lett.* **45**, 1502 (1980).
¹⁸J. A. Marquesee and J. M. Deutch, *J. Chem. Phys.* **75**, 5179 (1981).
¹⁹A. L. Kholodenko and K. F. Freed, *J. Chem. Phys.* **80**, 900 (1984).
²⁰M. Daoud, P. Pimons, W. H. Stockmayer, and T. Witten, *Macromolecules* **16**, 183 (1984).
²¹T. Ishinabe, *J. Phys. A* **18**, 3181 (1985).
²²V. Privman, *Macromolecules* **19**, 2377 (1986).
²³V. Privman, *J. Phys. A* **19**, 3287 (1986).
²⁴B. Derrida and H. Saleur, *J. Phys. A* **18**, 1075 (1985).
²⁵B. Duplantier and H. Saleur, *Phys. Rev. Lett.* **59**, 539 (1987).
²⁶P. H. Poole, A. Coniglio, N. Jan, and H. E. Stanley, *Phys. Rev. Lett.* **60**, 1203 (1988).
²⁷F. Seno and A. L. Stella, *J. Phys. (Paris)* **49**, 739 (1988).
²⁸F. Seno and A. L. Stella, *Europhys. Lett.* **7**, 605 (1988).
²⁹C. Vanderzande, *Phys. Rev. B* **38**, 2865 (1988).
³⁰F. Seno, A. L. Stella, and C. Vanderzande, *Phys. Rev. Lett.* **61**, 1520 (1988); B. Duplantier and H. Saleur, *ibid.* **61**, 1521 (1988).
³¹A. R. Massih and M. A. Moore, *J. Phys. A* **8**, 237 (1975).
³²Y. Shapir and Y. Oono, *J. Phys. A* **17**, L39 (1984).
³³Y. Shapir, A. Guha, and H. A. Lim (unpublished).
³⁴H. A. Lim, A. Guha, and Y. Shapir, *J. Phys. A* **21**, 773 (1988).
³⁵A. Guha, H. A. Lim, and Y. Shapir, *J. Phys. A* **21**, 1043 (1988).
³⁶I. S. Chang, A. Guha, H. A. Lim, and Y. Shapir, *J. Phys. A* **21**, L559 (1988).
³⁷H. A. Lim, *J. Phys. A* **21**, 3783 (1988).
³⁸N. Metropolis, A. W. Rosenbluth, M. N. Rosenbluth, A. H. Teller, and E. Teller, *J. Chem. Phys.* **21**, 1087 (1953).
³⁹P. H. Verdier and W. H. Stockmayer, *J. Chem. Phys.* **36**, 227 (1962).
⁴⁰E. Eisenrigler, K. Kramer, and K. Binder, *J. Chem. Phys.* **77**, 6296 (1982).
⁴¹P. M. Lam, *Phys. Rev. B* **36**, 6988 (1987).
⁴²A. Berretti and A. D. Sokal, *J. Stat. Phys.* **40**, 483 (1985).
⁴³H. A. Lim, unpublished results.
⁴⁴P. Grassberger, *Phys. Lett.* **89A**, 381 (1982).